K-Stabilized High-Oxygen-Coverage States on Rh(110): A Low-Pressure Pathway to Formation of Surface Oxide

Sebastian Günther,*,† Friedrich Esch,‡ Marco del Turco,‡,# Cristina Africh,‡,# Govanni Comelli,‡,# and Maya Kiskinova*,§

Department Chemie, Ludwig-Maximilians Universtät München, Butenandtstrasse 11 Haus E, 81377 München, Germany, and Laboratorio TASC-INFM, Area Science Park, 34012 Trieste, Department of Physics and Center of Excellence for Nanostructured Materials, University of Trieste, 34127 Trieste, and Sincrotrone Trieste, Area Science Park, 34012 Trieste, Italy

Received: February 25, 2005; In Final Form: April 21, 2005

Using scanning tunneling microscopy, low-energy electron diffraction, and X-ray photoelectron spectroscopy, we studied the evolution of the structure and chemical state of a Rh(110) surface, modified by K adlayers and exposed to high O_2 doses at elevated temperatures. We find that oxygen coadsorption on the K-covered Rh(110) leads to massive reconstruction of the Rh(110) surface. Stable reconstructed (10×2) and (8×2) segmented phases with a local coverage of more than two oxygen atoms per surface Rh atom were observed. Formation of surface oxide, which coexists with the (10×2) and (8×2) segmented adsorption phases, is evidenced at the highest O_2 doses. The development of strongly reconstructed adsorption phases with oxide-like stoichiometry and surface oxide under UHV conditions is explained in terms of the stabilization of the (1×2) reconstruction and promotion of O_2 dissociation by the K adatoms.

1. Introduction

In the attempts to understand the reaction mechanism of many industrially important oxidation catalytic reactions, the knowledge about the actual microscopic chemical state of the metal catalyst is essential. After the pioneering paper on CO oxidation on Ru(0001),[1] which showed that the oxide (RuO_2) is the active phase in realistic catalytic conditions, exponentially increasing experimental and theoretical studies have exploited the oxidation mechanisms of the 4d and 5d transition metals (TMs), looking for correlations between the catalytic activity and the oxidation state of the catalyst. Important steps toward oxide formation are the dissociative adsorption of O_2, involving development of several adsorption phases with increasing oxygen coverage. It is followed by the incorporation of oxygen into the metal (Me) substrate lattice, which often leads to an organized O−Me−O trilayer structure, called surface oxide, ending with the growth of a crystalline bulk oxide.[2] According to the recent comprehensive theoretical studies for Ru(0001), Pd(111), Rh(111), Rh(100), and Ag(111) surfaces, the oxygen starts to penetrate subsurface above a certain critical adsorption coverage, which increases with increasing O−TM adsorption bond strength.[3] The formation of the surface oxide is favored, because the adsorption bond is weakened above the critical oxygen coverage to an extent that subsurface bonding, involving also local expansion of the lattice, is energetically more favorable. In the frame of thermodynamic considerations the stability of the surface oxide is determined by the chemical potential of oxygen at which the Gibbs free energies of the chemisorption and the surface oxide cross. If the crossing point is at a chemical potential lower than that for bulk oxide formation, the surface oxide is a stable equilibrium phase. Otherwise the surface oxide can be only kinetically stabilized. The differences are determined not only by the nature of the metal substrate but also by the surface orientation. For Rh, e.g., the surface oxide is not a stable equilibrium phase on the (111) surface,[4] but it is stable on the more open (100) surface.[5]

So far, most of the studies were carried out with closed packed surfaces, where the maximum coverage of adsorbed O is found to be one oxygen atom per surface metal atom (Me), i.e., a MeO stoichiometry. This is not the case for open surfaces, e.g., Pt(110) and Rh(110), where the spontaneous or O-induced (1×2) missing-row reconstruction favors the formation of segmented ($n \times 2$) adsorption phases with more than two oxygen atoms per first-layer metal atom, i.e., a MeO_x stoichiometry with $x \geq 2$.[6,7] The results on the Pt(110)-(1×2) oxidation demonstrated that the O-(12×2) adsorption state with a stoichiometry close to PtO_2 is more stable than the surface oxide trilayer.[6] Thus, according to ref 6, for the reconstructed Pt(110)-(1×2) surface the oxidation pathway does not require a surface oxide precursor, because the Gibbs free energy of the chemisorption state and the surface oxide cross at an oxygen chemical potential where the bulk oxide is already stable.

On the contrary, our recent studies show that the oxidation of Rh(110) follows the oxidation route via formation of a stable hexagonal RhO_2 surface oxide, which is characterized by a c(2×4) low-energy electron diffraction (LEED) pattern and distinct Rh 3d and O 1s core level peaks.[8,9] This c(2×4) surface oxide phase coexists with the high-coverage O-(2×1)p2mg and O-c(2×8) adsorption phases and traces of the ($n \times 2$) segmented phase.[9] The Rh(110) surface has a very rich oxygen adsorption phase diagram, including also ($1 \times n$) and (10×2) reconstructions.[7,10]

The Rh oxidation studies referred to above are performed by exposure of atomically clean surfaces to either molecular

* To whom correspondence should be addressed. Phone: +39-040-3758549. Fax:.+39-040-3758565. E-mail: sebastian.gunther@elettra.trieste.it (S.G.); kiskinova@elettra.trieste.it (M.K.).
† Ludwig-Maximilians Universtät München.
‡ Laboratorio TASC-INFM.
# University of Trieste.
§ Sincrotrone Trieste.

10.1021/jp050988p CCC: $30.25
Published on Web 05/25/2005

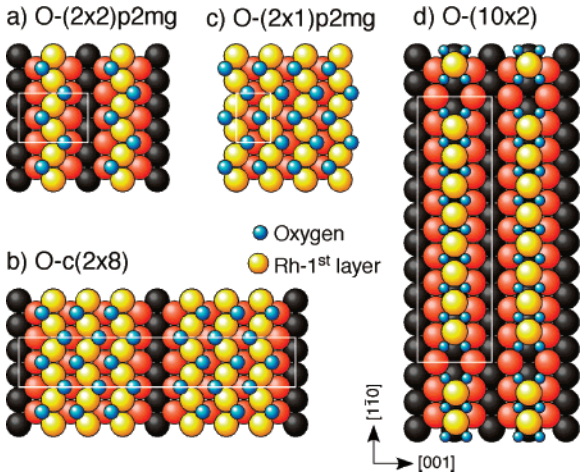

Figure 1. Hard sphere models of several oxygen adsorption structures on Rh(110): (a) O-(2 × 2)p2mg with $\theta_O = 0.5$ ML, (b) O-c(2 × 8) with $\theta_O = 0.75$ ML, (c) (2 × 1)p2mg with $\theta_O = 1$ ML, (d) O-(10 × 2) with $\theta_O = 0.9$ ML. The small spheres represent the oxygen atoms bonded to two first-layer Rh(I) atoms and one second-layer Rh(II) atom.

($p_{O_2} > 10^{-4}$ mbar) or atomic ($p_O \leq 10^{-6}$ mbar) oxygen at elevated temperatures ($T > 500$ K).[4,5,9] These studies showed that the gas ambient affects the oxidation rate and to a certain extent the lateral homogeneity of the oxide film.[9] However, the oxidation steps involve the same adsorption and surface oxide phases, which are believed to represent the phases formed during catalytic oxidation reactions as well. The present scanning tunneling microscopy (STM) study, supported by LEED and X-ray photoelectron spectroscopy (XPS), demonstrates that not only the oxidation rate but also the oxidation pathway can change in the presence of foreign adatoms on the surface, which are commonly used as additives in catalysis.

2. Experimental Section

The experiments were performed with variable-temperature STM (Omicron VT-STM) hosted in a UHV chamber, equipped with an Ar^+ ion gun, a gas inlet system, and an LEED−AES apparatus for controlling the sample surface composition. The Rh 3d and O 1s core level spectra were used as fingerprints of the actual chemical state of the Rh(110) surface. They were measured at the ESCA microscopy and SuperESCA beamlines at the synchrotron laboratory in Trieste. All experiments were carried out under the same reaction conditions, and the structure of the adsorbed layers was always verified by LEED.

The Rh(110) sample was cleaned by Ar^+ sputtering, followed by cycles of exposure to O_2 and annealing (up to 1100 K) until the surface showed a sharp (1 × 1) LEED pattern and no traces of surface impurities. The K coverage was evaluated by correlation of the LEED patterns to the K_{LMM}/Rh_{MNV} (AES) or K 2p/Rh 3d (XPS) intensity ratios, based on a previous calibration, where the K evaporation rate was monitored by a quartz microbalance.[11]

Atomic oxygen was provided by an electron cyclotron resonance plasma source (Tectra) and dosed at chamber pressures in the 10^{-6} mbar range. Since the cracking efficiency has not been calibrated, only the upper limits for the atomic O exposures are quantified.

3. Results

A. O and K Adsorption Phases on Rh(110). For the sake of clarity we shortly describe the O and K adsorption phases, which are related to the results of the present study. Figure 1 shows the structural models of the O adsorption phases formed for O coverages ≥0.5 monolayer (ML), by exposing the Rh-(110)-(1 × 1) surface to oxygen at different temperatures. One ML is equal to the number of Rh atoms of the Rh(110)-(1 × 1) surface. At $T > 400$ K oxygen induces consecutive (1 × n) missing-row reconstructions.[10] Independently of the surface structure the O adatoms always occupy 3-fold sites along the [1$\bar{1}$0] rows in a zigzag arrangement. Considering only the first-layer atoms, this gives a RhO stoichiometry for all adsorption phases. The O atoms are bonded to two surface Rh(I) atoms and one second-layer Rh(II) atom. The (1 × 2) reconstruction strengthens the O bonding with the Rh atom from the second layer. At $\theta_O = 0.5$ ML a (2 × 2)p2mg adsorbate phase on a (1 × 2) missing-row-reconstructed Rh(110) surface is formed (Figure 1a). The accommodation of more than 0.5 ML of oxygen on the (1 × 2) surface cannot compensate the strong O−O repulsion arising from adding another atom in the next nearest fcc site along the [1$\bar{1}$0] row, which would lead consecutively to $RhO_{1.5}$ and RhO_2 stoichiometries. Apparently it is more favorable to preserve the RhO stoichiometry, and the accommodation of more than 0.5 ML is accompanied by a surface deconstruction. The increasing fraction of the (1 × 1) surface is illustrated by the O-c(2 × 8) structure in Figure 1b. The (2 × 1)p2mg structure (Figure 1c) with 1 ML of oxygen requires complete deconstruction to a Rh(110)-(1 × 1) surface. At elevated temperatures ($T > 400$ K) this occurs only under high-pressure conditions or an exposure to atomic oxygen. At 300 K, when the sample does not reconstruct, only the (2 × 1)p2mg structure with 1 ML of oxygen is formed.

Considering only the Rh atoms from the top layer, the segmented (10 × 2) structure in Figure 1d has stoichiometry $RhO_{2.25}$ and hosts an absolute O coverage of 0.9 ML. The segments consist of eight Rh atoms and are terminated with vacancies, created by the ejection of Rh atoms from the [1$\bar{1}$0] rows. The removal of one Rh atom on each side of the segments allows ∼10% expansion of the Rh−Rh distance in the [1$\bar{1}$0] direction, so the eight Rh atoms occupy about nine substrate sites. However, this structure can be formed only starting from an O-(2 × 2)p2mg/Rh(110) surface and adsorbing additional oxygen at $T < 250$ K followed by a short anneal, to keep the substrate mobility low. In contrast to the O-(12 × 2) structure on Pt(110)-(1 × 2), the (10 × 2) structure on the Rh(110)-(1 × 2) surface is metastable and exists due to kinetic hindrance. It converts spontaneously to c(2 × 2n) (with $n \geq 4$) phases at elevated temperatures.[7] That is why, during oxidation of an atomically clean Rh(110) surface at $T > 500$ K, the dense O-(2 × 1)p2mg and c(2 × 2n) adsorption phases are the dominant phases coexisting with the surface oxide, which has a hexagonal c(2 × 4) symmetry.[8,9]

K adsorption on the Rh(110) surface induces the same (1 × n) missing-row reconstructions. Missing-row reconstructive alkali-metal adsorption is a general phenomenon occurring also on other fcc(110) transition metals.[12] Increasing the K coverage up to ∼0.12 ML induces consecutive (1 × 4), (1 × 3), and (1 × 2) reconstructions with K adatoms, embedded in the (1 × 2) missing-row troughs. At K coverage higher than 0.12 ML the surface reverts back to (1 × 3) and (1 × 4), the latter hosting the highest K coverage of 0.19−0.23 ML at 300 K.[11] At $T > 300$ K the K adatoms are very mobile, do not form long-range ordered structures, and are usually not visible with STM.[13]

B. Structure of the O + K Coadsorption Phases with High Oxygen Coverage. The adsorption of oxygen on K-covered Rh(110) at elevated temperatures results in a wealth of ordered

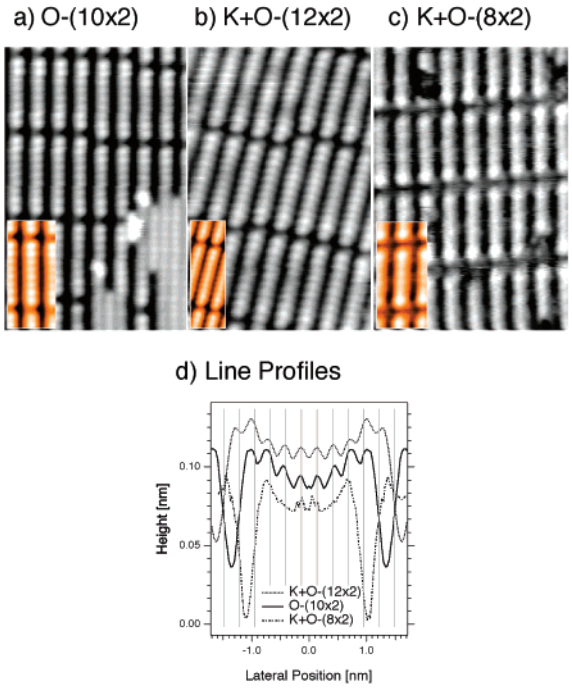

Figure 2. STM images (6.3 × 9.8 nm^2) taken at 300 K: (a) O-(10 × 2) on Rh(110), prepared by exposure of an O-(2 × 2)p2mg/Rh(110) surface to 26 L of O_2 at 200 K followed by a fast anneal to 540 K (V = +0.63 V and I = 1.0 nA); (b) K + O-(12 × 2) region on Rh(110), obtained after exposure of a 0.12 ML K-(1 × 2)/Rh(110) surface to 30 L of O_2 at 520 K (V = +0.2 V and I = 0.4 nA); (c) K + O-(8 × 2) region on Rh(110) obtained after exposure of a K-(1 × 2)/Rh(110) surface to 23 L of O_2 at 570 K, followed by several H_2 titration (23 L at 660 K) and reoxidation (23 L at 570 K) cycles (V = +0.08 V and I = 0.22 nA); (d) STM line profiles along the [1$\bar{1}$0] rows of O-(10 × 2), K + O-(12 × 2), and K + O-(8 × 2) structures, taken from configurationally averaged images shown in the insets of (a)−(c). The profiles have been made symmetrical by averaging with the mirrored counterpart. The vertical lines indicates the substrate atom positions in the [1$\bar{1}$0] rows of the clean Rh(110) surface.

structures.[11,14] A distinct feature is that, independently of the K coverage, the K + O phases with high oxygen coverage always involve segmented (1 × 2) reconstructions. This holds for θ_K > ~0.03 ML and high O_2 doses (up to 60 L) at temperatures of 500−700 K, typically used in the studies of the oxidation of a K-free Rh(110) surface.[8,9] These segmented (n × 2) reconstructions are of the same type as the O-(10 × 2) in Figure 1d, and will therefore be called (10 × 2)-type reconstructions in the following. The length n of the unit cell, however, depends on the formation conditions and shows a certain variability;[14] each segment inside the unit cell is constituted by n − 2 Rh atoms.

In the following, we consider the K + O mixed phases, formed by very high O exposures on K-covered Rh(110) with $\theta_K \geq 0.12$ ML. Figure 2 shows the STM images of the (10 × 2)-type structures, formed by saturation with oxygen of O-(2 × 2)p2mg/Rh(110) and 0.12 ML K-(1 × 2)/Rh(110) surfaces. They appear very similar, consisting of segments with varying lengths, but predominantly built by 8 (a), 10 (b), and 6 (c) Rh atoms, leading to (10 × 2), (12 × 2), and (8 × 2) unit cells, respectively. As will be discussed below, the most uniform (8 × 2) phase in Figure 3c is obtained after titration with H_2 and reoxidation cycles. The only sensible difference is that the O-(10 × 2) structure, formed on the K-free surface, contains many defects (mostly O-(2 × 1)p2mg islands). These defects are unavoidable, since the preparation requires low mobility of the Rh atoms, conditions that also favor the formation of the more stable O-(2 × 1)p2mg phase by the ejected Rh atoms. In contrast, the K + O-(10 × 2)-type structures are stable and can be prepared almost free of defects by dosing oxygen at 550−600 K. Preparation involving reduction−oxidation cycles at 570−660 K narrows the length distribution, favoring the formation of the ordered (8 × 2) structure with shorter segments. The STM line profiles along the [1$\bar{1}$0] rows of the O-(10 × 2), K + O-(12 × 2), and K + O-(8 × 2) structures (Figure 2d) indicate that also in the presence of K the Rh atoms within the segments are expanded in the [1$\bar{1}$0] direction by ~10%. Due to the poorer quality of the image the line scans of the (8 × 2) structure do not show atomic resolution. However, the positions of the maxima at the end of the (8 × 2) segments coincide with the maxima of the corresponding Rh atoms from the (10 × 2) segments, which confirms the Rh−Rh expansion.

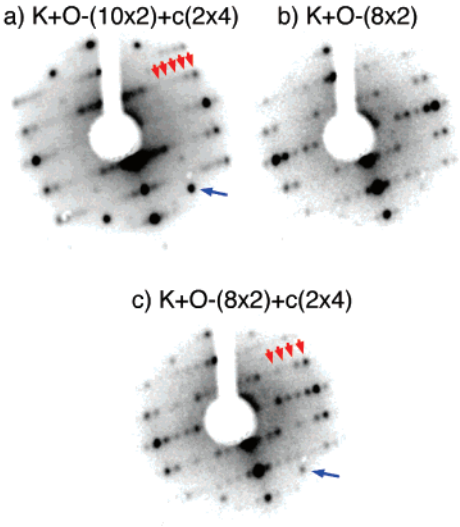

Figure 3. LEED patterns of dense K + O adlayers: (a) after exposure of the ~0.17 ML K-(1 × 3)/Rh(110) surface to 23 L of O_2 at 300 K and 46 L of O_2 at 570 K (E_{kin} = 52 eV); (b) after exposure of the surface in (a) to 23 L of H_2 at 660 K (E_{kin} = 78 eV); (c) after reoxidation of the surface in (b) with 110 L of O_2 at 660 K (E_{kin} = 78 eV). The arrows at the bottom of (a) and (c) indicate the spot belonging to the c(2 × 4) structure. The array of arrows in (a) and (c) is a guide indicating the changes in the distance and number of spots due to conversion of the (10 × 2) structure to the (8 × 2) structure.

C. Formation of Surface Oxide under UHV Conditions. The K + O adlayer structures, obtained after a K/Rh(110) surface with θ_K > 0.15 ML is exposed to very high O_2 doses at T > 600 K and after further reduction/oxidation cycles, show extra spots in the LEED patterns which cannot simply be attributed to the formation of K + O adsorption phases.

Figure 3a shows the LEED pattern, obtained by exposing a K-(1 × 3)/Rh(110) surface with θ_K = 0.17 ML to 23 L of O_2 at 300 K, followed by 46 L of O_2 at 570 K. A distinct feature of the LEED pattern is the appearance of additional spots of a c(2 × 4) symmetry along with those of the (10 × 2) structure. Exposing this surface to ~23 L of H_2 at 660 K leads to removal of the c(2 × 4) spots and conversion of the (10 × 2) structure to the (8 × 2) one, displayed in Figure 3b. Additional exposure to 110 L of O_2 at 660 K sharpens the (8 × 2) pattern and restores the c(2 × 4) spots, which have vanished during H_2 titration. This result also indicates that the (8 × 2) arrangement should be energetically more favorable than the (10 × 2) one. Most likely the segmentation process is kinetically constrained, and this can be overcome by partial reduction of the O atoms: the Rh surface atoms are relieved and can rearrange into a more open structure, providing more favorable sites for accommoda-

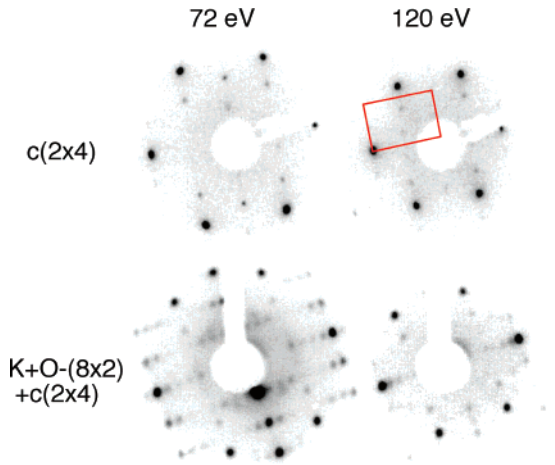

Figure 4. LEED patterns obtained at $E_{kin} = 72$ and 120 eV from the surface oxide phase on K-free Rh(110) (top) and from the Rh(110) surface from Figure 3c with high K coverage of 0.17 ML after exposure to 110 L of O_2 at 660 K (bottom).

tion of the dense K + O layer. Since the O adsorption state is preserved and saturated after the reoxidation, the (10 × 2) to (8 × 2) transition results in an effective increase of the number of O atoms per surface Rh atom from 2.25 to 2.33.

The second very important result is the development of the c(2 × 4) spots, which belong to a new surface phase, coexisting with the (10 × 2) or the (8 × 2) chemisorption phases. This is confirmed by the variations in the spot intensities with changing electron kinetic energy. The c(2 × 4) diffraction patterns appear very similar to those obtained from the surface oxide on the K-free Rh(110).[8] Figure 4 compares the changes with the electron kinetic energy of the c(2 × 4) pattern from the surface oxide, formed on a K-free surface, and the c(2 × 4) extra spots coexisting with the (8 × 2) pattern. The intensity of the coexisting c(2 × 4) spots reflects the hexagonal symmetry of the surface oxide, clearly seen in the pattern measured at 120 eV. This indicates that the hexagonal c(2 × 4) and the (8 × 2) structures are two different phases, the c(2 × 4) one being identical to the oxide on the K-free surface.

We should stress that, on the K-covered Rh(110) surface with $\theta_K > 0.15$ ML, the c(2 × 4) surface oxide forms under UHV conditions, i.e., after adsorption of 140 L of O_2 at 660 K, whereas the oxidation of the Rh(110) surface requires O_2 pressures $>10^{-4}$ mbar and exposures >10000 L at $T > 700$ K or exposures >200 L to atomic oxygen at $p_O = 10^{-6}$ mbar and $T > 500$ K. The extinction of the c(2 × 4) pattern during titration with H_2 (see Figure 3b) is in accordance with the high reactivity of the c(2 × 4) surface oxide phase, observed on a K-free Rh-(110) surface.[9] While the LEED experiments clearly demonstrate the existence of the c(2 × 4) phase, we failed with STM to resolve the structure in the areas presumably belonging to the c(2 × 4) phase. One possible reason is the very unstable tunneling condition in the presence of K, which worsens at very high K coverage, when the formation of a c(2 × 4) surface oxide is promoted. This also explains why no atomic resolution was obtained when the coexisting (8 × 2) regions were imaged.

Unambiguous proof that the coexisting c(2 × 4) structure reflects the formation of surface oxide is the O 1s and Rh $3d_{5/2}$ spectra measured on these surfaces and illustrated in Figure 5. Figure 5a−c displays the O 1s and the Rh 3d core level spectra of coadsorbed layers, representing the K + O-(10 × 2) and mixed (10 × 2) + c(2 × 4) phases. For the sake of comparison, the O 1s and Rh $3d_{5/2}$ spectra of the O-(10 × 2) adsorption structure and the K-free Rh(110) surface with

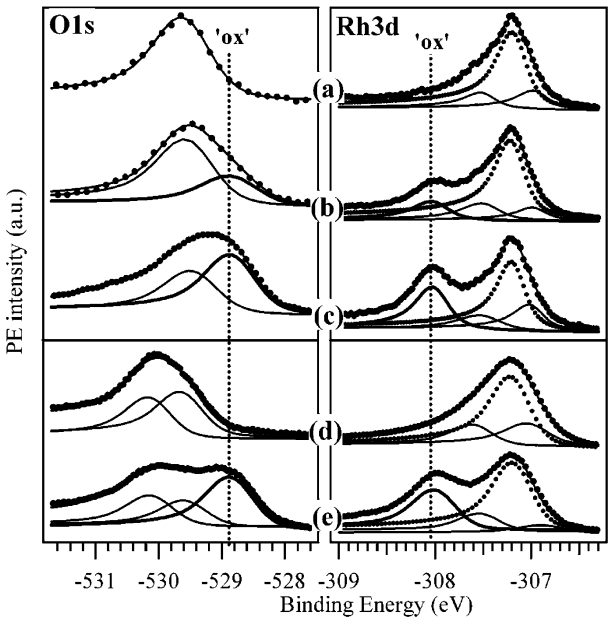

Figure 5. O 1s and Rh $3d_{5/2}$ spectra taken from the (a) K + O-(10 × 2) surface prepared by exposing a K-(1 × 2)/Rh(110) surface ($\theta_K = 0.12$ ML) to 57 L of O_2 at 570 K, (b) K + O-(10 × 2) + c(2 × 4) surface prepared by exposing a K-(1 × 4)/Rh(110) surface ($\theta_K = 0.19$ ML) to 67 L of O_2 at 570 K, (c) K + O-(10 × 2) + c(2 × 4) surface prepared by exposing a K-(1 × 4)/Rh(110) surface ($\theta_K = 0.21$ ML) to 60 L of O_2 at 300 K followed by an adsorption of 100 L of O_2 at 570 K, (d) O-(10 × 2) surface prepared by adsorbing 4 L of atomic O at 250 K on an O-(2 × 2)p2mg surface followed by a brief anneal to 540 K, and (e) c(2 × 4) surface oxide and coadsorbed phases on Rh(110) formed by exposure to 150 L of atomic oxygen at 520 K.

coexisting c(2 × 4) surface oxide and adsorption phases are also shown in Figure 5d,e.

The O 1s spectrum of the K + O-(10 × 2) phase formed by saturation of a 0.12 ML K-(1 × 2)/Rh(110) surface with oxygen at 570 K has a single component at 529.5 eV, compatible with the structural model of the segmented phase in Figure 1d. The metastable O-(10 × 2) structure formed on a K-free surface shows in addition a second component peaked at 530.1 eV. This binding energy can be attributed to oxygen adsorbed in the (2 × 1)p2mg islands always coexisting with the O-(10 × 2) structure (see Figure 2a). The corresponding Rh $3d_{5/2}$ spectra in Figure 5a,d are very similar, because the spectral resolution does not allow us to discriminate between the effect of the strain induced by the O adatoms and the effect of K coadsorption.

High O_2 exposure on Rh(110) covered with $\theta_K > 0.15$ ML leads to growth of another component in the O 1s spectrum at 528.9 eV (Figure 5b, marked as "ox"), in addition to the one at 529.5 eV. This low-energy O 1s component appears at the same binding energy as the oxide component due to photoemission from the surface oxygen atoms in the hexagonal oxide films on Rh single-crystal surfaces.[4,5,8,9] At this high K coverage the O 1s intensity does not saturate at ~0.9 ML, as in the case of low and moderate K coverage, but continues to grow, the contribution of the 528.9 eV peak becoming more pronounced. This is manifested by the significant increase of the oxide component in the O 1s spectrum from the mixed (10 × 2) + c(2 × 4) phase upon repetitive oxygen dosing (Figure 5c). In fact, the O 1s spectrum in Figure 5c resembles the O 1s spectrum in Figure 5e, measured in the earlier oxidation stages of the Rh(110) surface. The difference is in the presence of a high-binding-energy component in the latter, which accounts for the coexisting areas with nonsegmented adsorption phases, evi-

denced by both LEED and STM. The distinct high-binding-energy component that appears in the Rh $3d_{5/2}$ spectrum is an indisputable proof for the oxide nature of the coexisting c(2 × 4) structure observed for high-coverage K + O adlayers. This component is present only in the Rh $3d_{5/2}$ spectra of the surface oxide phases formed on the three low-index Rh surfaces and reflects the highly O coordinated Rh atoms in these phases.[4,5,8,9]

4. Discussion

The prerequisite to formation of segmented, O-induced (10 × 2)-type adsorption phases is the interaction of oxygen with already (1 × 2) missing-row-reconstructed fcc(110) surfaces. According to the DFT calculations the lower coordination number of the metal atoms on the reconstructed surface shifts the center of the d band upward, thus effectively increasing the O adsorption bond strength[15] This explains the O-induced (1 × *n*) missing-row reconstructions of Rh(110) and other 3d transition-metal surfaces.[16] The (10 × 2)-type structures can be considered as a more advanced stage of reconstruction. They also involve expansion of the Me−Me interatomic distance along the [1$\bar{1}$0] direction, which is supposed to weaken the O−O repulsive interactions and even increase attractive O−O interactions.[17] The lattice distortion allows an increase of the maximum number of O atoms per surface metal atom: while on non-reconstructed Rh(110) the stoichiometry is one O atom per first-layer Rh atom, in the O-(10 × 2) structure it is 2.25 O atoms per first-layer Rh atom. Thus, the (10 × 2)-type adsorption phases can accommodate about the same absolute amount of oxygen as the nonreconstructed (1 × 1) surface having a more than 2 times lower density of surface metal atoms. However, the massive restructuring involved in the formation of the O-induced (10 × 2)-type adsorption phases imposes kinetic constraints. If there is no significant energy gain with respect to the other deconstructed phases, the (10 × 2)-type phases will thus only be metastable.

In the case of Pt(110) the (1 × 2) reconstruction is the equilibrium state of the surface and the energy gain for the formation of a segmented O-(12 × 2) structure to accommodate close to 0.92 ML of oxygen is apparently higher than the adsorption of a similar amount of oxygen on a deconstructed (1 × 1) surface. Therefore, a substrate deconstruction due to oxygen adsorption does not take place. In the case of Rh(110), the deconstruction of the 0.5 ML O-(1 × 2)/Rh(110) surface prevails, leading to c(2 × 2*n*) adsorption phases with further increasing O coverage. In fact, during the oxidation of Rh(110) only traces of (10 × 2)-type segments can be seen in the intermediate stage, where c(2 × 8), c(2 × 10), and (2 × 1)-p2mg are the dominant adsorption phases coexisting with the surface oxide.

The change of the energy balance to segmented (10 × 2)-type phases in the presence of K is a result of several contributions. The first is the stabilization of the (1 × 2) reconstruction due to the energetically favorable adsorption site of K in the missing-row trough and due to the screening of the O−O repulsion as a result of the attractive K−O interactions. Indeed, independently of the initial K coverage and surface structure, the O coadsorption always first reverts the surface to (1 × 2), which undergoes further (10 × 2)-type reconstructions to accommodate high O coverage. The presence of K moves the energy balance toward the (10 × 2)-type reconstructions, because on such very open surfaces the K and O adsorption states are more effectively stabilized via K−O interactions. Inside the (1 × 2) troughs and the vacancies between the segments the plane of the spatial charge distribution of the K 4s valence states is closer to the plane of the O adatoms located along the [1$\bar{1}$0] rows, whereas on the (1 × 1) troughs the K adatoms are well above the plane of the O adatoms. This scenario is in accordance with the picture of the K adatom bonding on transition-metal surfaces.[18,19] It is mainly of electrostatic nature and does not affect sensibly the width and energy position of the transition-metal d bands. This extra charge, built up around the K adatoms, preserves a high O_2 dissociative adsorption rate, the effect becoming even more pronounced at high K coverage. The continuous accumulation of oxygen after the saturation of the K + O-induced (10 × 2)-type phases leads consequently to the formation of surface oxide under UHV conditions, i.e., using ∼200 times lower O_2 doses. Furthermore, in contrast to the pure O-Rh(110) system, the presence of K stabilizes a very open reconstructed surface. This provides easier access to the Rh atoms of the second and third layers, undoubtedly facilitating the buildup of surface oxide.

5. Conclusions

Complementary STM, LEED, and XPS studies have shown that the oxidation rate and the oxidation pathway of the Rh(110) surface can be easily modified by the presence of K adlayers. The main result of the present investigation is that the K adlayers promote massive restructuring of the Rh(110) surface and formation of segmented (10 × 2)-type adsorption structures with local RhO_x stoichiometry, with $x > 2$. These structures easily accommodate high oxygen coverage and mediate the formation of surface oxide, a process which readily occurs under UHV conditions. The present results are direct evidence for the complexity of realistic systems, where a rich variety of self-organized nanostructures may form and coexist during oxidation reactions. Since the alkali metals are important promoters for many catalytic oxidation reactions, we show that the reactive phase cannot be predicted simply by bridging the pressure gap, i.e., without taking into account the pressure-induced change in the structural complexity.

Acknowledgment. This work has been supported by MIUR under the programs FIRB 2001 (Contract No. RBNE0155X7) and COFIN 2003, as well as by EU Contract No. NMP3-CT-2003-505670 (NANO2).

References and Notes

(1) Over, H.; Kim, Y. D.; Seitsonen, A. P.; Lundgren, E.; Schmid, M.; Varga, P.; Morgante, A.; Ertl, G. *Science* **2000**, *287*, 1474.

(2) Reuter, K.; Sheffler, M. *Appl. Phys.* **2004**, *A 78*, 793 and the references therein.

(3) Todorova, M.; Li, W. X.; Ganduglia-Pirovano, M. V.; Stampfl, C.; Reuter, K.; Scheffler, M. *Phys. Rev. Lett.* **2002**, *89*, 96103.

(4) Gustafson, J.; Mikkelsen, A.; Borg, M.; Lundgren, E.; Köhler, L.; Kresse, G.; Schmidt, M.; Varga, P.; Yuhara, J.; Torrelles, X.; Quiros, C.; Andersen, J. N. *Phys. Rev. Lett.* **2004**, *92*, 126102.

(5) Gustafson, J.; Mikkelsen, A.; Borg, M.; Andersen, J. N.; Lundgren, E.; Klein, C.; Schmidt, M.; Varga, P.; Köhler, L.; Kresse, G.; Kaspar, N.; Stierle, A.; Dosch, H. *Phys. Rev. B*, in press.

(6) Li, W. X.; Österlund, L.; Vestergaard, E. K.; Vang, R. T.; Matthiesen, J.; Pedersen, T. M.; Lægsgaard, E.; Hammer, B.; Besenbacher, F. *Phys. Rev. Lett.* **2004**, *93*, 146104.

(7) Vesselli, E.; Africh, C.; Baraldi, A.; Comelli, G.; Esch, F.; Rosei, R. *J. Chem. Phys.* **2001**, *114*, 4221.

(8) Esch, F.; Kresse, G.; et al. Manuscript in preparation.

(9) Dudin, P.; Barinov, A.; Gregoratti, L.; Kiskinova, M.; Esch, F.; Dri, C.; Alfrich C.; Comelli, G. Submitted for publication to *J. Phys. Chem.*

(10) Comelli, G.; Dhanak, V. R.; Kiskinova, M.; Prince, K. C.; Rosei, R. *Surf. Sci. Rep.* **1998**, *32*, 165 and references therein.

(11) Hoyer, R. Diploma Thesis, Uni Hannover, 2000.

(12) Barnes, C. J. Adsorbate induced reconstruction of f.c.c.{110} Surfaces. In *The Chemical Physics of solid surfaces*; King, D. A., Woodruff, D. P., Eds.; Elsevier: Amsterdam, 1994; Vol. 7, Chapter 13..

(13) Doyen, G.; Drakova, D.; Barth, J. V.; Schuster, R.; Gritsch, T.; Behm, T.; Ertl, G. *Phys. Rev. B* **1993**, *48*, 1738.

(14) Günther, S.; et al. Manuscript in preparation.

(15) Mavrikakis, M.; Hammer, B.; Norskov, J. K. *Phys. Rev. Lett.* **1998**, *81*, 2819.

(16) Besenbacher, F.; Norskov, J. K. *Prog. Surf. Sci*. **1993**, *44*, 5.

(17) Helveg, S.; Lorensen, H. T.; Horch, S.; Lægsgaard, E.; Stensgaard, I.; Jacobsen, K. W.; Norskov, J. K.; Besenbacher, F. *Surf. Sci*. **1999**, *430*, L533.

(18) Coadsorption, Promoter and Poisons. In *The Chemical Physics of Solid Surfaces and Heterogeneous Catalysis*, King, D. A., Woodruff, D. P., Eds.; Elsevier: New York, 1993; Vol. 6, Chapters 1−3 and 7−9.

(19) Kiskinova, M. *Poisoning in Catalysis Based on Surface Science Concepts in Studies in Surface Science an Catalysis*; Elsevier: New York, 1992; Vol. 70, Chapters 4.1 and 6−8 and references therein.